

## Solid-Liquid Interface Characterization by Photoelectrochemical Measurement of Optical Absorption

Jeffrey C. Buchholz

*Physics Department, General Motors Research Laboratories, Warren, Michigan 48090*

(Received 10 April 1978)

The electronic structure of a platinum/electrolyte interface is determined by photoelectrochemical measurement of optical absorption processes. Photoemission into the electrolyte shows the electrode surface to be metallic at cathodic potential while thin semiconducting oxide layers are observed at anodic potentials. Internal photoemission at the metal/oxide interface indicates the Fermi level to be at midgap for the oxide which has a band gap of 3.1 eV.

This Letter presents a direct characterization of the electronic structure of the platinum/acid electrolyte interface. The physical processes of photoemission into an electrolyte,<sup>1</sup> photogalvanic electrochemical processes for semiconductors,<sup>2</sup> and internal photoemission<sup>3</sup> at a solid/solid interface are all observed. These processes are combined for the first time to determine the band gap and band positions of a very thin (0.1–0.6 nm), semiconducting, anodic oxide film at a metal/liquid electrolyte interface. These data are also used to determine the position of the metal Fermi level relative to electronic levels in the electrolyte for a metallic platinum surface.

The solid/liquid electrolyte interface has not previously been very well characterized experimentally, particularly when compared to the solid/gas interface. Tremendous advances have been made in applying various electron spectroscopies to solid/gas interface problems.<sup>4</sup> These techniques are unfortunately not applicable to the solid/liquid interface. Thus optical techniques such as reflectance<sup>5</sup> and ellipsometry<sup>6</sup> are usually employed to study the electronic properties of the solid/liquid interface. Although these measurements probe the electronic structure of the interface, there are several problems that make them less than ideal. Firstly, when very thin surface layers, on the order of angstroms thick, are being studied, the substrate contribution to the measured optical properties is very large. Thus, the experiment consists of measuring a very small change in a large reflected signal. Secondly, it is often difficult to interpret the measurement in terms of the fundamental electronic properties of the surface layer. One needs, for example, to extract the optical constants by a Kramers-Kronig analysis which involves assumptions about quantities such as film thickness which may be unknown.

The approach described here is essentially an optical absorption measurement, but be-

cause of the way in which the absorption is detected, only the contributions of specific absorption processes are measured. This removes some of the uncertainties of the optical measurements and makes the interpretation of the results much more straightforward. Since the surface to be studied is part of an electrochemical cell, any process or photoinduced reaction at the interface leading to charge transfer can be readily detected as a change in the cell current. The primary processes which contribute to this photoelectrochemical current are shown in Fig. 1. Additional processes such as photochemistry in the solution are possible but are not applicable to the system described here.

Direct photoemission of electrons from the sol-

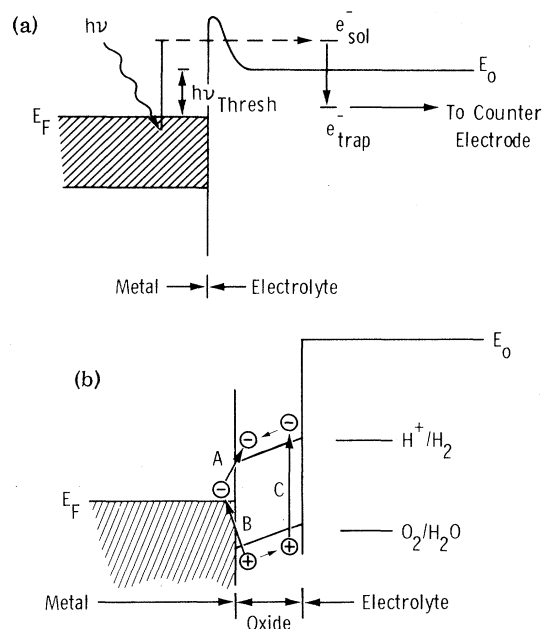


FIG. 1. Interfacial energy level diagrams. (a) Photoemission from a metal into an electrolyte. (b) Metal/oxide/electrolyte interface at a potential anodic with respect to flat-band potential.

id into the electrolyte<sup>1</sup> is shown schematically in Fig. 1(a) for emission from a metallic electrode. The potential variation at the interface arises from the electrochemical dipole layer as well as image-potential effects. At cathodic potentials where photoemission is observed (below the potential of zero charge at which point there is no preferred orientation of the water dipoles at the surface), the electrochemical dipole layer is expected to produce a potential barrier at the interface. Although the barrier shape will be heavily influenced by image-potential effects, the barrier thickness is determined primarily by the electrochemical dipole layer, which is only several water molecules thick, since the high dielectric constant of the water beyond this dipole layer makes the image potential fall off much more rapidly than in vacuum experiments. Thus photoexcited electrons with sufficient energy and proper momentum can tunnel through the barrier into the solution at photon energies less than the vacuum work function. In the solution the electrons become solvated, quasifree electrons before finally being trapped, by a  $\text{H}_3\text{O}^+$  ion in acid solution, and discharged at the counter electrode which completes the cell circuit.

An alternate source of photocurrent exists at a semiconducting electrode as shown in Fig. 1(b). Electrons or holes generated by absorption of radiation of energy greater than the band gap [process C in Fig. 1(b)] can react with electron-accepting or -donating redox species in solution. These redox levels can be thought of as deep acceptor and donor trap levels within the water band gap. These photogalvanic electron-transfer processes are the basis of recent work in photoelectrochemical energy conversion devices.<sup>7</sup> The band bending in the semiconducting layer as shown in Fig. 1(b) results in holes coming to the interface to react with electron-donating species. If the electrode potential,  $E_0 - E_F$  in Fig. 1(b), is changed to favor migration of electrons to the interface, reaction with electron-accepting species will be observed. Thus currents of either sign can be observed due to process C, the sign of the current changing at the flat-band potential.

If the semiconducting layer is sufficiently thin, internal photoemission processes such as A and B in Fig. 1(b) also contribute to carrier generation. For thick oxides, these processes would not contribute to the photoelectrochemical current because of electron-hole recombination before the charge carriers reach the electrochemical interface. For platinum, with oxide thick-

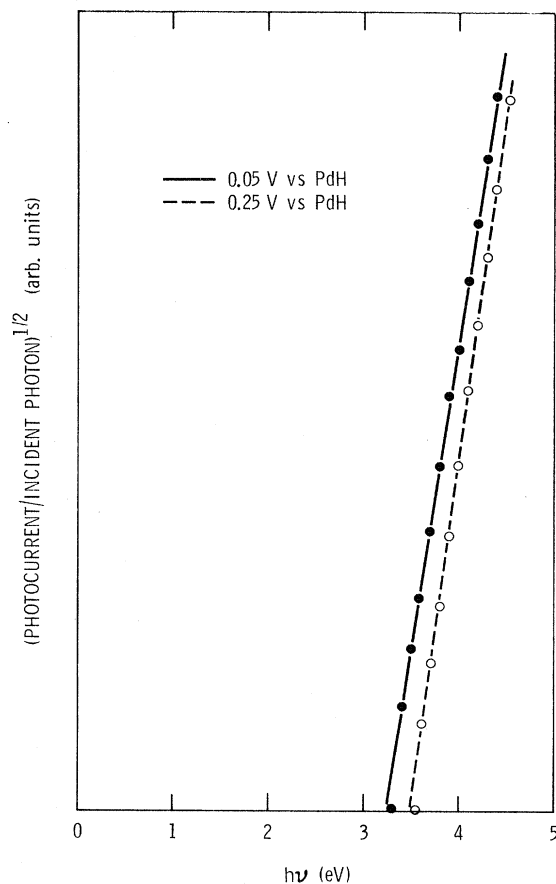


FIG. 2. Photoemitted current for a platinum electrode at two cathodic potentials.

nesses reported from 0.2 to about 0.5 nm depending on potential,<sup>8</sup> all of these absorption processes are expected to contribute to the measured photocurrent.

Photocurrent data for a platinum foil electrode in 1N  $\text{H}_2\text{SO}_4$  electrolyte are shown in Figs. 2 and 3 for several different electrode potentials. The potentials are measured against a PdH reference electrode in the same solution. In the language of Fig. 1, the reference electrode provides a redox energy level (deep trap) fixed relative to  $E_0$ , the energy zero in the electrolyte. The PdH reference electrode level<sup>9</sup> is in fact 50 mV below the  $\text{H}^+/\text{H}_2$  level indicated. The electrode was illuminated by a 1000-W xenon arc lamp filtered through a prism monochromator. Slit widths of 2.5 mm were used for high throughput. This resulted in an energy resolution of about 0.2 eV over the wavelength range of interest. Chopped illumination at about 3 Hz was used so that the current between the test and counter electrodes could be synchronously detected to eliminate any

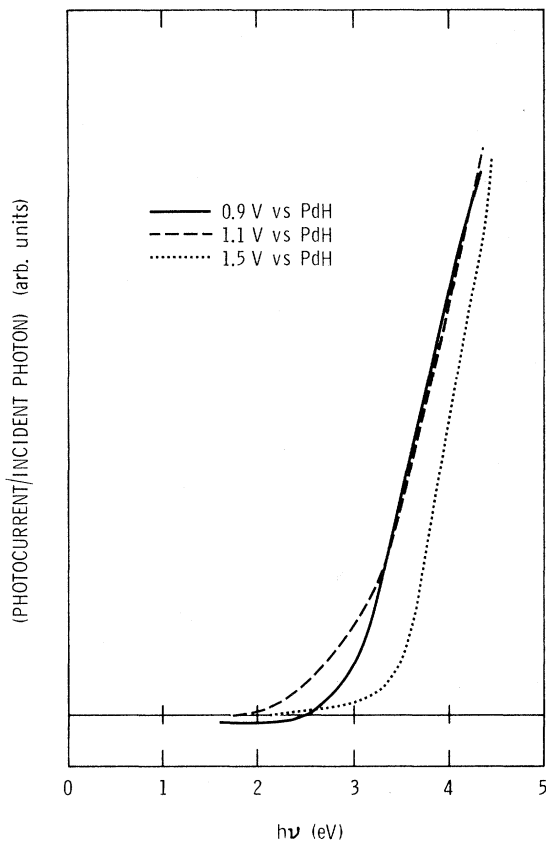


FIG. 3. Photocurrent for anodic potentials. The sign of the 0.9- and 1.5-V currents has been reversed.

dc electrochemical background. The electrode potential was held fixed relative to the reference during the measurement by a commercial potentiostat. Cyclic voltammetry showed the electrode to be clean by present electrochemical standards.

The photoemission current measured at two cathodic potentials is shown in Fig. 2. The data have been plotted assuming a dependence on photon energy of the form  $I = A(h\nu - h\nu_{\text{thresh}})^2$  to allow extrapolation to zero current to obtain the photoemission threshold. The dependence of the photocurrent threshold on electrode potential is evidence that the current is in fact photoemission from a metallic surface. From the model in Fig. 1(a), the emission threshold  $h\nu_{\text{thresh}} = E_0 - E_F$  will vary directly with the electrode potential. This is observed in the dependence of the threshold shown in Fig. 2 and other data over the potential range from  $-0.1$  to  $+0.3$  V vs PdH. The threshold energy shifts by the change in electrode potential. These data establish the quasifree, solvated electron level,  $E_0$ , to be  $3.2$  eV above the metal Fermi level at an electrode potential of

$0.0$  V vs PdH. Equivalently,  $E_0$  is  $3.15$  eV above the hydrogen reference electrode redox level,  $H^+/H_2$ , in the electrolyte [see Fig. 1(b) for the relative position of solution levels].

At anodic potentials, from  $+0.8$  V vs PdH to  $1.5$  V vs PdH, a considerably more complicated behavior of the photocurrent threshold is observed. A continuous variation of threshold with potential does not exist but rather three different thresholds are observed for various electrode potentials. This indicates the presence of semiconducting surface films as described in Fig. 1(b). There is hysteresis in the photocurrent threshold behavior with electrode potential. This is because the surface oxide film is growing to increased thickness as the potential is raised but does not decrease in thickness when the potential is lowered until it desorbs completely at about  $0.8$  V vs PdH. Figure 3 shows the three photocurrent thresholds that are observed for various electrode potentials and potential histories. The data for  $+0.9$  V were measured as the potential was raised from  $0.0$  to  $2.0$  V, that is, for increasing oxide growth. The data for  $+1.5$  and  $+1.1$  V were measured as the potential was decreased from  $2.0$  V. In this case the oxide film thickness is constant until the film is removed at about  $+0.8$  V.

If the electrode potential is raised to  $+0.9$  V vs PdH from lower potentials, the surface, which had shown metallic behavior, develops an absorption threshold at  $2.5 \pm 0.2$  eV as shown in Fig. 3. The direction of the current is opposite to that for photoemission and corresponds to holes reacting with donors in the solution. This  $2.5$ -eV threshold is attributed to absorption in an adsorbed oxygen phase, possibly resulting in photo-stimulated desorption of the adsorbed oxygen. Raising the potential further, to greater than about  $1.2$  V vs PdH, causes this threshold to disappear and a two-threshold system to develop. The thresholds of  $1.6 \pm 0.2$  eV and  $3.1 \pm 0.2$  eV, obtained by an extrapolation analysis as used in Fig. 2, still correspond to reactions involving holes at the interface. If the potential is increased to  $2.0$  V vs PdH which increases the oxide layer thickness ( $0.3$  nm at  $1.4$  V), then returned to  $1.5$  V vs PdH for measurement, predominantly the  $3.1$ -eV threshold is observed (Fig. 3,  $V = 1.5$  V). Measurements cannot be made at  $2.0$  V vs PdH because of interfering gas evolution. This  $3.1$ -eV threshold is attributed to absorption of band-gap radiation and reaction of the hole with the electrolyte [process C in Fig. 1(b)]. The  $1.6$ -eV

threshold is due to generation of holes by internal photoemission such as process *B* in Fig. 1(b). The contribution of this process is decreased on the return sweep from 2.0 V vs PdH because the increased oxide film thickness causes an increase in electron-hole recombination before the carriers reach the oxide/electrolyte interface. Thus the data for 1.5 V vs PdH shown in Fig. 3 are almost exclusively from band-gap absorption above the 3.1-eV threshold.

The photocurrent reverses direction when the potential is decreased to below 1.2 V vs PdH. This corresponds to electrons in the conduction band being transferred to acceptors in the solution. The flat-band potential is thus about 1.2 V vs PdH. Below 1.2 V vs PdH the photocurrent is dominated by a 1.6-eV threshold current (see Fig. 3,  $V=1.1$  V). This current is attributed to generation of electrons in the conduction band by internal photoemission such as process *A* in Fig. 1(b). The dominance of this process over band-gap absorption (process *C*) is probably a result of contributions from a considerable depth in the metal since both the optical penetration depth and the electron mean free path at these energies are much greater than the oxide film thickness.

The approximate equivalence of the threshold energies for processes *A* and *B* leads to an assignment of the Fermi level in the oxide film to about midgap.

Although electron photoemission could contribute to the photocurrent at anodic potentials, the expected threshold would be at a much higher energy than the thresholds that are observed. Since  $E_0$  is 3.2 eV above the  $H^+/H_2$  level (or, approximately, the PdH level), the threshold for photoemission from the oxide Fermi level, the minimum possible threshold, would be 4.3 eV at a potential of 1.1 V vs PdH. This is considerably larger than what is observed.

An alternative explanation of the observed threshold behavior would assign the 1.6- and 3.1-

eV thresholds to absorption of band-gap radiation in two different semiconducting phases. This model would require rapid conversion back and forth between the two phases, however, since for oxides grown at 2.0 V vs PdH, the 3.1-eV threshold dominates above 1.2 V vs PdH and the 1.6-eV threshold below. Such a rapid interconversion seems unlikely. In addition, both phases would have to have the same flat-band potential since both currents reverse direction at the same potential.

In summary, the models for the platinum/electrolyte interface shown in Fig. 1 provide reasonable agreement with the observed photocurrent data. Photoemission into the electrolyte from the metallic surface at cathodic potentials determines  $E_0$  to be about 3.2 eV above the hydrogen potential ( $H^+/H_2$ ) in the electrolyte. At anodic potentials, two surface phases are observed. An initial phase, probably adsorbed oxygen, has an absorption threshold of about 2.5 eV. A second, oxide phase behaves like a semiconductor with a band gap of 3.1 eV with its Fermi level at midgap.

<sup>1</sup>J. K. Sass, R. K. Sen, E. Meyer, and H. Gerischer, *Surf. Sci.* **44**, 515 (1974).

<sup>2</sup>H. Gerischer, *J. Electroanal. Chem.* **58**, 263 (1975); H. Gerischer, E. Meyer, and J. K. Sass, *Ber. Bunsenges.* **76**, 1191 (1972).

<sup>3</sup>R. Williams, in *Semiconductors and Semimetals*, edited by R. K. Willardson and A. C. Beer (Academic, New York, 1970), Vol. 6.

<sup>4</sup>See, for example, E. W. Plummer, in *Springer Topics in Applied Physics*, edited by R. Gomer (Springer, Berlin, 1975), Vol. 4.

<sup>5</sup>See, for example, K. Naegele and W. J. Plieth, *Surf. Sci.* **50**, 64 (1975).

<sup>6</sup>M. Stedman, *Symp. Faraday Soc.* **4**, 64 (1970).

<sup>7</sup>See, for example, M. S. Wrighton, A. B. Ellis, and S. W. Kaiser, in *Solar Energy* (The Electrochemical Society, Inc., New York, 1976).

<sup>8</sup>S. H. Kim, W. K. Paik, and J. O'M. Bockris, *Surf. Sci.* **33**, 617 (1972).

<sup>9</sup>J. P. Hoare, *Gen. Mot. Eng. J.* **9**, 14 (1962).